



**HAL**  
open science

## Visualization of toner ink adsorption at bubble surfaces

Zachery Emerson, Thomas Bonometti, Gopal Krishnagopalan, Steve Duke

► **To cite this version:**

Zachery Emerson, Thomas Bonometti, Gopal Krishnagopalan, Steve Duke. Visualization of toner ink adsorption at bubble surfaces. Tappi Journal, 2006, vol. 5, pp.10-16. hal-00906399

**HAL Id: hal-00906399**

**<https://hal.science/hal-00906399>**

Submitted on 19 Nov 2013

**HAL** is a multi-disciplinary open access archive for the deposit and dissemination of scientific research documents, whether they are published or not. The documents may come from teaching and research institutions in France or abroad, or from public or private research centers.

L'archive ouverte pluridisciplinaire **HAL**, est destinée au dépôt et à la diffusion de documents scientifiques de niveau recherche, publiés ou non, émanant des établissements d'enseignement et de recherche français ou étrangers, des laboratoires publics ou privés.



## Open Archive TOULOUSE Archive Ouverte (OATAO)

OATAO is an open access repository that collects the work of Toulouse researchers and makes it freely available over the web where possible.

This is an author-deposited version published in : <http://oatao.univ-toulouse.fr/>  
Eprints ID : 9413

**To cite this version** : Emerson, Zachery and Bonometti, Thomas and Krishnagopalan, Gopal and Duke, Steve Visualization of toner ink adsorption at bubble surfaces. (2006) TAPPI Journal, vol. 5 (n° 4). pp. 10-16. ISSN 0734-1415

Any correspondance concerning this service should be sent to the repository administrator: [staff-oatao@listes-diff.inp-toulouse.fr](mailto:staff-oatao@listes-diff.inp-toulouse.fr)

# Visualization of toner ink adsorption at bubble surfaces

ZACHERY I. EMERSON, THOMAS BONOMETTI, GOPAL A. KRISHNAGOPALAN AND STEVE R. DUKE

**ABSTRACT:** Flotation deinking involves interactions between ink particles and bubble surfaces. These interactions are very difficult to observe directly or to quantify in bench-scale experiments or mill operations. That means it is difficult to evaluate effects of process conditions such as bubble size and solution chemistry on deinking efficiency. This paper presents images and measurements of toner ink interactions with bubble surfaces in laboratory-scale flotation processes. Stable adsorption of toner ink occurred at surfaces of stationary and suspended bubbles for several system chemistries. We used high magnification and high temporal resolution digital videos to quantify interactions of toner particles with flowing and stationary bubbles in bubble flow facilities. Large (>200 micron), flat toner particles adsorbed to bubble surfaces by single contact points. Smaller toner particles formed very stable complexes in fatty acid chemistries. Desorption of toner ink from bubble surfaces was not observed, even for vigorous flows. Bubbles were observed to be fully covered with toner after 4 min of residence time in the suspending bubble flow facility. Initial estimates indicate that bubbles with diameters of approximately 1 mm carry more than 1 mg of ink per bubble.

**Application:** A laboratory technique is described that allows quantitative and systematic study of froth flotation and dissolved-air flotation processes important to the paper recycling industry.

This paper describes qualitative and quantitative results from an optical visualization method that provides observations and measurements of toner ink adsorption processes at the surfaces of stationary and moving bubbles. The technique provides a means for systematic study of flotation processes and enhancement of the understanding of the mechanisms of ink-bubble interactions. The optical methods build upon the methods developed in our laboratories for the study of flexographic and offset inks and stickies [1-3].

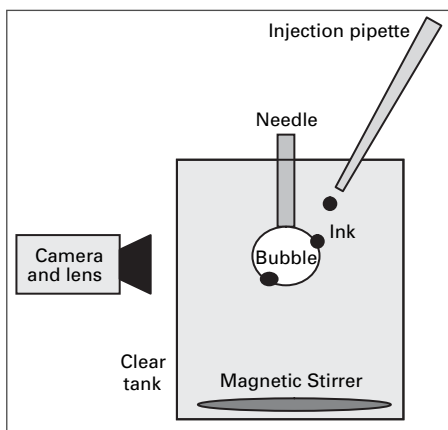
Effective adsorption of contaminants at bubble surfaces is important to froth flotation deinking processes and to dissolved air flotation processes. Contaminants such as inks, adhesives, and other additives are removed from recycled fiber in froth flotation cells. Hydrophobic suspended solids, including ink particles, attach to rising bubbles and are incorporated into a frothy layer at the top of the flotation cell. The froth layer is skimmed and dewatered. The dewatered contaminant sludge is disposed of or burned. Many contaminants, particularly small and hydrophilic inks and additives, are removed from secondary fiber by washing. These washing processes require large quantities of water. The wash water (filtrate from wash deinking) contains contaminants that must be removed before the water can be reused or discharged. A typical method available

for cleaning this wash water is dissolved air flotation (DAF).

Different ink types respond differently to flotation processes [4,5]. Oil-based inks such as offset inks have hydrophobic properties, so they generally respond efficiently to flotation processes. The water-dispersible nature of flexographic inks causes them to respond poorly to flotation separations, so chemical aids are added to increase the separation efficiency. Toner inks are nonimpact inks that are used in photocopying and laser printing. In these printing processes the resin binder of the ink is fused to the paper surface by light or heat. Toner ink particles can be difficult to remove from the fiber surface due to this binding, and they form large flat flakes upon repulping. The size of the released particles depends on a number of factors, including the pH in the repulping system [6]. The resin binder base of toner is very hydrophobic, so toner responds well to flotation from a surface chemistry standpoint. However, the large size of the particles is thought to increase the hydrodynamic strain on an adsorbed particle [4]. Dorris found that the optimum particle size for high flotation efficiency of nonimpact inks falls in the range of 60 to 100 microns [7]. Results presented in this paper focus primarily on experiments conducted with toner inks.

The technology, chemistry, and theory associated with flotation deinking and

dissolved air flotation are well developed and efficient for many recycling systems [8, 9]. However, the demand for recycled fiber, coupled with the availability of new printing technologies and the prevalence of new contaminant varieties, has brought about an increased need to better understand flotation processes at a fundamental level. Successful flotation depends upon a combination of surface chemistry and fluid mechanics, with the central phenomenon being the interactions of solid particles with bubble surfaces. Heindel [10] reviews the theoretical microprocesses that result in ink removal: particle capture, attachment by sliding, three-phase contact, and stability. The microprocesses are not easily measured or effectively modeled because they are complex relations dependent on the system hydrodynamics and chemistry and the properties of the particles (inks) and bubbles [11]. The underlying phenomena associated with interactions of contaminant particles and bubble surfaces can be affected through control of solution chemistry (fatty acids, calcium, surfactants, pH, and other additives), particle size and morphology, bubble size, flow characteristics, temperature, and other parameters. The optical methods described in this paper and elsewhere [1, 2,12-15] offer a means of determining and measuring the small-scale fundamental processes that govern the complex full-scale processes.



**1. Stationary bubble facility. Ink is injected onto the stationary bubble. The magnetic stirrer produces agitation.**

## EXPERIMENTAL

Thorough descriptions of the flow facilities and imaging systems are in Davies et al. [1] and Davies and Duke [2].

### Stationary bubble facility

Figure 1 illustrates the stationary bubble facility. In this setup, a medical-grade flat tip needle was placed in a 2 L transparent tank. The tank was filled with water or a surfactant solution. The needle was connected to a syringe pump that allowed a small volume of air to be supplied such that a stable bubble was created at the tip of the needle. The needle assembly can be oriented so that the needle points up or down. Solutions that contained contaminants (toner ink particles) were injected with a pipette onto the bubble surface and the interactions were imaged using the camera and lens system described later.

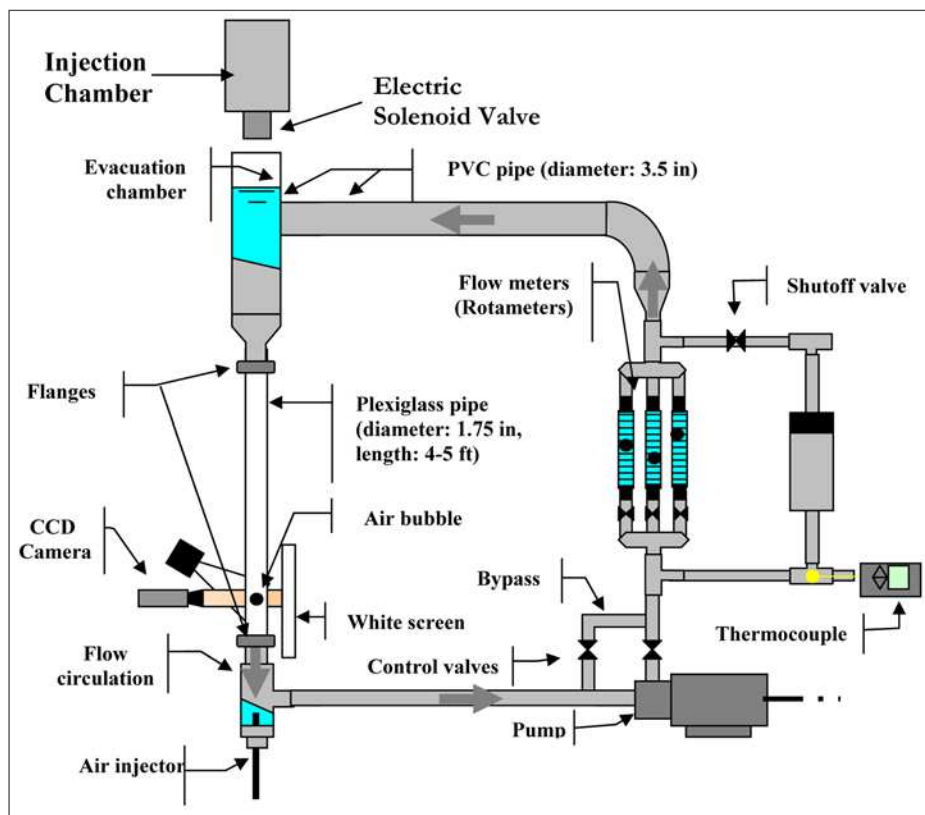
A magnetic stirrer bar in the stationary bubble tank allowed testing of the stability of adsorbed particles. Visualizations were obtained of the particles adsorbed to the bubble in the flow field generated for various stirrer rotation speeds. The degree of agitation (the vigor of the flow field or the level of turbulence) is expressed by the tank Reynolds number,  $Re_{Tank}$ , and is defined as:

$$Re_{Tank} = \frac{D_{Tank} u_B}{\nu} \quad (1)$$

where  $D_{Tank}$  is the diameter of the tank,  $\nu$  is the kinematic viscosity of the solution (assumed to be that for water), and  $u_B$  is the bulk velocity in the tank due to stirring. The bubble Reynolds number is defined as:

$$Re_{Bubble} = \frac{D_{Bubble} u_B}{\nu} \quad (2)$$

where  $D_{Bubble}$  is the diameter of the bubble. The bulk velocity was determined by measuring frame-to-frame displacements



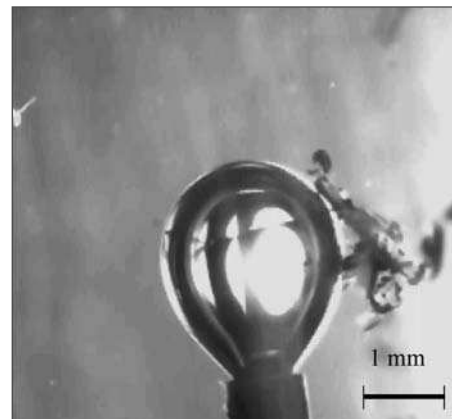
**2. Suspending bubble flow facility. A counter flow of water suspends a bubble in view of the camera. Ink is injected at the top of the column.**

of toner ink particles that did not contact the bubble. An average displacement distance obtained for several particles was multiplied by the frame rate to obtain the bulk velocity.

### Bubble suspending flow facility

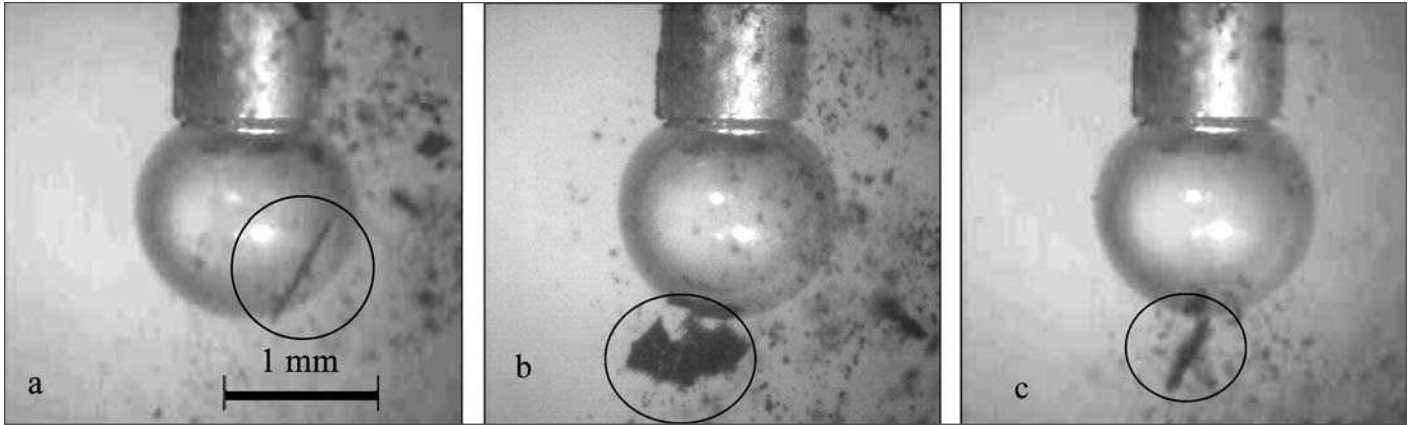
Figure 2 shows the bubble suspending flow facility. In this setup a surfactant solution was circulated by a pump through a flow loop. One or more bubbles were released from a needle into the section of the flow loop where the solution flows down through a clear, vertical column. The counter flow of water suspended the bubbles in the field of view of the imaging system. The flow rate of solution is such that the flow field around the suspended bubble matches that of a rising bubble of an identical size. The toner particles or other contaminants were introduced at the top of the column and were carried by the flowing solution to contact the bubbles. The interactions between the bubbles and ink particles were then recorded by the high speed imaging system.

The imaging column is a plexiglass pipe, held in place with flanges so that different columns may be used. A larger pipe (38 mm diameter) is generally used to reduce the wall effects. The air is injected through medical grade needles and supplied directly from a compressed air cylinder. The flow from the cylinder

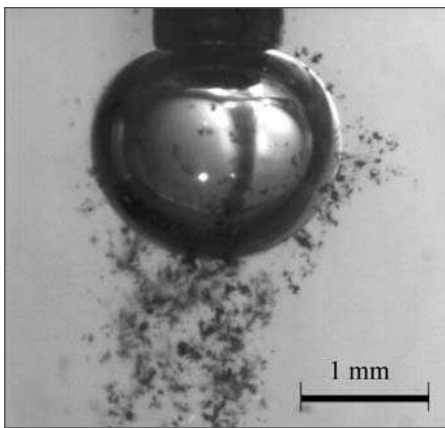


**3. Image of the adsorption of toner ink in water at a pH of 9.5.**

and the needle size can each be altered to control the size and number of suspended bubbles. The water pump is a 1/8 hp Cole-Palmer magnetic drive pump; it is rated at 3200 rpm and delivers 14 gal/min with 10 feet of head. The rotometers are polysulfone direct-reading, in-line flow-meters with 316 stainless steel floats. We arranged three flow-meters in parallel to measure three different flow ranges: 0.1–1.0 gal/min, 0.2–2.0 gal/min, and 2.0–20.0 gal/min. At the top of the column is a holding chamber that allows bubbles to leave the flow loop before reaching the pump. At the bottom of this chamber are vertical 1/4 in. tubes that reduce velocity profiles in the flow field



**4. Images of the adsorption of toner ink in sodium oleate solution at pH = 9.5. A large planar toner particle (a) approaches the bubble, (b) attaches to the bubble by two sharp contact points, and (c) spins stably attached at the bottom of the bubble.**



**5. Image of small networked toner particles adsorbed onto the surface of a stationary bubble.**

entering the imaging column. Davies determined the flow to be fully developed at a distance of about 1 foot down the length of the column [1]. Therefore, all imaging of the column occurs along the lower half of the column. For 1 mm diameter bubbles, typical velocities of water were 16.0 cm/s (volumetric flows were 30.5 L/min). The flow rate of solution is such that the flow velocity around the suspended bubble matches the rise velocity for a bubble of the same size [1].

#### **Imaging and analysis systems**

We used a Kodak Motion Corder high-speed CCD camera system to obtain images of the ink-bubble interactions. This system can operate at speeds of up to 1000 frames per second. Most of the work presented here was performed at 250 frames per second with an image resolution of 512-by-480 pixels. The shutter speed was 4 milliseconds. A combination of back incandescent lighting and front halogen lighting was used.

We used a Video Zoom Microscopic VZM 300I lens (from Edmund Scientific) for high magnification analysis of the bubble surface. It has a magnification of up to 3 times, and a minimum field of view of 4 mm<sup>2</sup>. For much of this work the microscope lens was operated at a magnification of 1.5 times and a field of view of 25 mm<sup>2</sup>. Typical magnification was 7 μm per camera pixel for the stationary bubble tank and 26 μm per pixel for the flow column. Visualizations were also obtained with various Nikon lenses, which provided lower magnification but larger fields of view.

Image data was acquired in uncompressed bitmap format using the Kodak camera software. Video sequences (movies) were assembled in AVI format. All measurements and image processing calculations were based on still images and employed appropriate software packages (primarily HL Image++ and Image Tool).

#### **Ink and system solution preparation**

Flotation system solutions from fatty-acid chemistry were prepared in a manner similar to that used by Dorris and Nguyen [16]. A typical solution for fatty-acid chemistry contained 100 mg/L calcium chloride and 100 mg/L sodium oleate. We added sodium hydroxide to adjust pH. Water used for the experiments was deionized and distilled. Some experiments were conducted with “clear” water, which means that no chemicals were added except for sodium hydroxide to adjust pH.

The toner ink used in these experiments was obtained from a Hewlett-Packard toner inkjet cartridge 92298-A for a LaserJet-4 printer. The toner ink

before application is a blend of poly(methyl-methacrylate) and poly(acrylic acid) binder with carbon black pigment.

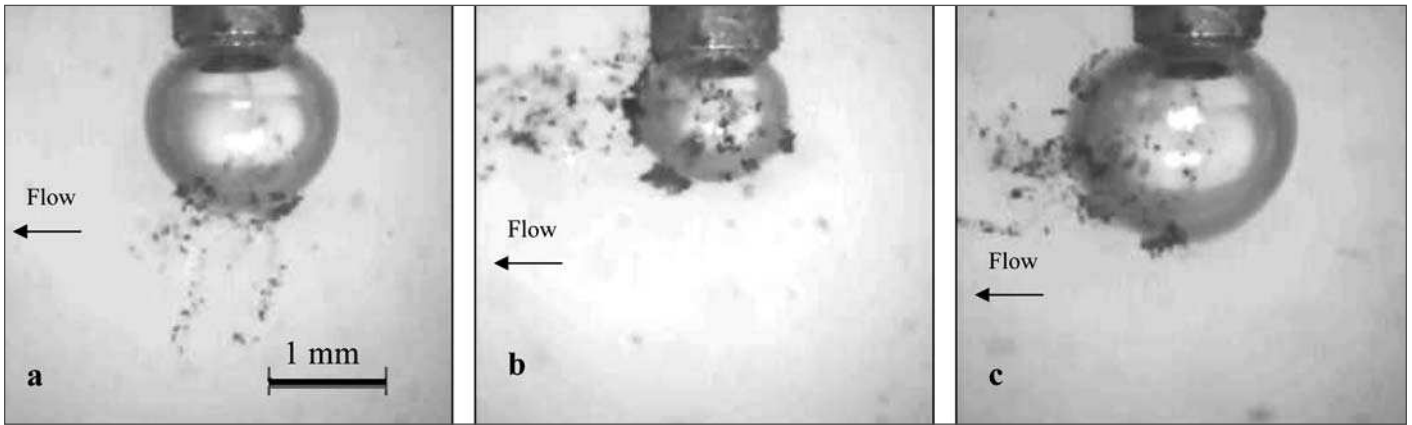
Transparencies were printed with toner ink and then soaked in distilled-deionized water for 2 hours. The ink was scraped off of the surface of the transparencies and collected at the bottom of the soaking vessel, in a manner similar to that used by Paulsen et al. [12]. Approximately 0.26 g of ink particles were in each sample of concentrated ink suspension removed from the collection vessel by pipette. The samples were then injected into the stationary facility. For the suspending bubble facility, the ink and water mixture was poured rapidly into the top of the flow loop. Approximately 2.5 g of ink was introduced into the loop for each run. Studies were conducted in the absence of fiber.

## **RESULTS AND DISCUSSION**

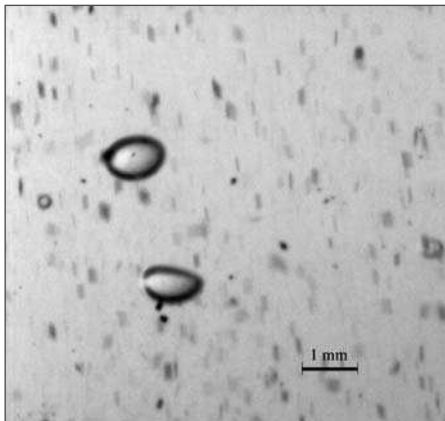
### **Toner adsorption imaging for stationary bubbles**

Toner particles readily adsorbed on bubble surfaces in the stationary bubble tank. Video sequences showed flat toner particles ranging from 20 μm to 400 μm adsorbing to bubbles approximately 1 mm in diameter. Toner ink adsorbed onto bubbles in clear water and in fatty-acid chemistry solution. In fatty-acid solution, toner formed fairly stable networks of particles attached to one another. Key observations from the video sequences are illustrated as still frames in Figs. 3 through 6.

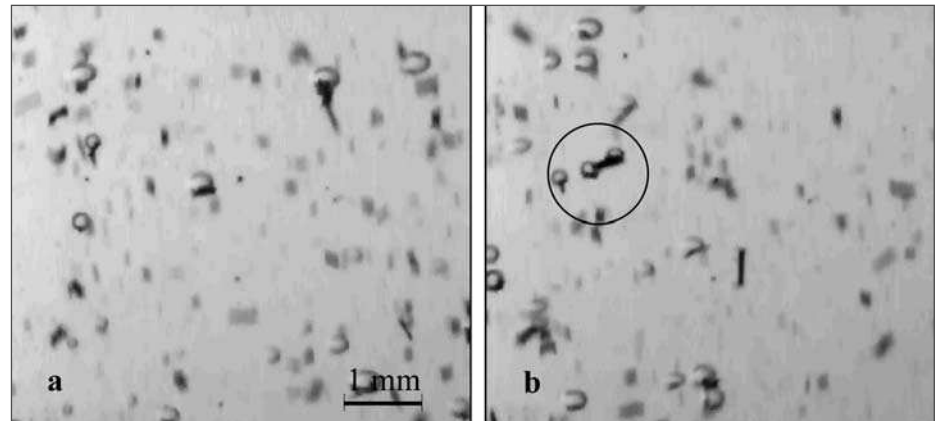
The image in **Fig. 3** is from a video sequence taken for toner ink particles injected into the stationary bubble tank. The image was taken for clear water at a



6. Images of adsorbed toner networks in the presence of flow generated by stirrer. (a)  $Re_{Tank} = 900$ ,  $Re_{Bubble} = 20$ . (b)  $Re_{Tank} = 3000$ ,  $Re_{Bubble} = 70$ . (c)  $Re_{Tank} = 7000$ ,  $Re_{Bubble} = 160$ .



7. Image of suspended bubbles in clear water with adsorbed toner ink particles.



8. Images of toner ink injection in sodium oleate solution with pH of 9.5. (a) Several small bubbles during a toner injection. (b) Two small bubbles attached to a single toner particle.

pH of 9.5. The images in Fig. 4 show the adsorption of a large ( $400\ \mu\text{m}$  by  $200\ \mu\text{m}$ ) toner ink particle onto a bubble in fatty-acid chemistry. Figure 4a shows a large, planar particle as it collides with the bubble. The particle attached to the bubble by two small contact points (Figure 4b), and then spun in place due to the injected fluid motion (Figure 4c). Paulsen et al. [12] also observed that large toner particles form stable attachments to bubble surfaces via sharp contact points.

Figure 5 shows a number of adsorbed toner ink particles on the surface of a bubble in fatty-acid chemistry. A large network of ink particles has formed, trailing from the surface of the bubble. This network of particles assembled very quickly after the particles were injected onto the bubble surface. The network phenomenon was only observed in the fatty-acid (calcium-soap) chemistry. The video sequences reveal that particles first adsorbed to the bubble surface and then the network built out from the adsorbed particles. The networks were not observed to develop in solution away from the bubble surface. Particles were observed to attach directly to the net-

work; other particles were observed to attach to the bubble surface and then move toward the network. We are investigating the formation and stability of these complexes, and their dependency on proximity to the bubble surface.

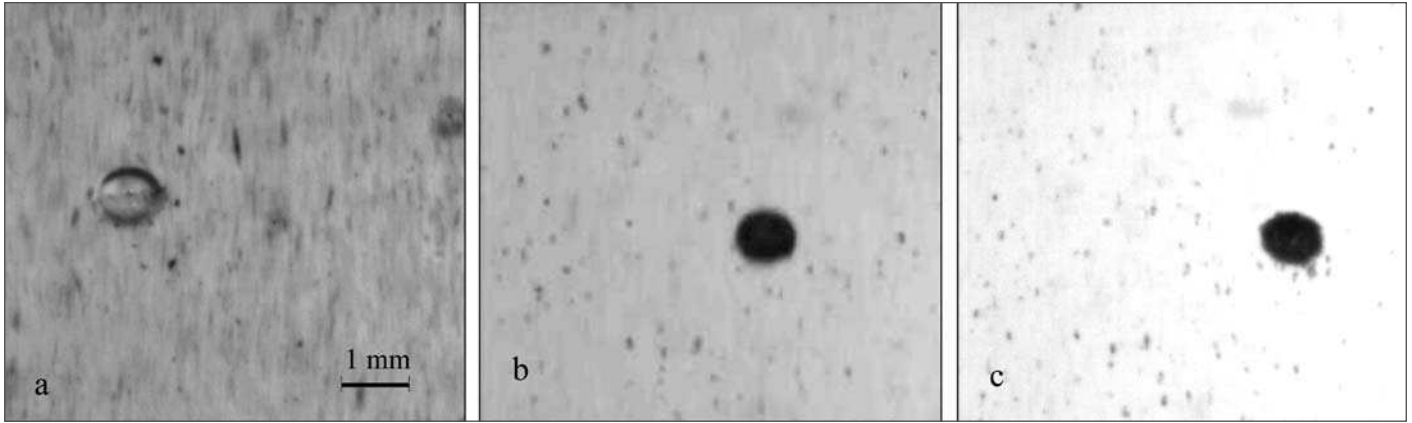
Figure 6 shows frames from a series of stability tests used to examine the strength of the toner ink adsorption. Figure 6a shows an adsorbed toner network with  $Re_{Tank} = 900$  and  $Re_{Bubble} = 20$ . Figure 6b is an adsorbed complex with  $Re_{Tank} = 3000$  and  $Re_{Bubble} = 70$ . Figure 6c shows a similar network in the presence of agitation yielding  $Re_{Tank} = 7000$  and  $Re_{Bubble} = 160$ . The image in Fig. 6c was taken just before the bubble became dislodged from the needle tip and left the field of view. Desorption of attached ink from the bubble surface was not observed, even for the highest level of mixing.  $Re_{Bubble}$  values in a deinking flotation cell are typically in the range of 1 to 100 [17].

#### Toner adsorption imaging for suspended bubbles

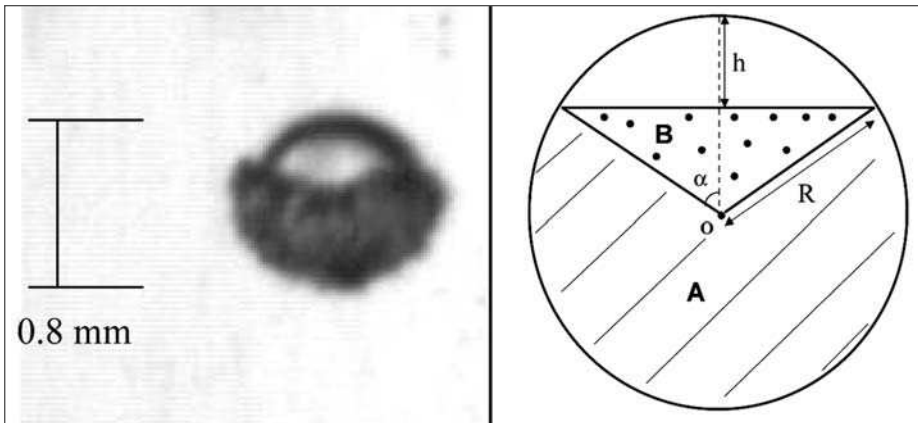
Toner ink readily adsorbed to bubbles suspended in the flow column. A typical video sequence began with a bubble sus-

pended in a flow of ink particles. Adsorbed toner quickly began to accumulate on the downstream side of the bubble surface. The ink coverage spread up the bubble surface until, in some cases, complete bubble coverage was observed. As the experiment progressed, the number of ink particles in the column decreased due to adsorption to bubble surfaces. Key observations from the video sequences are illustrated as still frames in Figs. 7-9.

Figures 7 and 8 show suspended bubbles with adsorbed toner ink attached. Figure 7 shows a pair of bubbles (approximately 1 mm in size) with adsorbed toner ink particles in calcium soap solution at a pH of 9.5. The ink is seen at the bottom of the bubbles. Figure 8 shows a selection of frames from an injection of toner into a column containing many small bubbles (0.25-1.0 mm diameter). Figure 8a shows several small bubbles with large adsorbed toner ink particles. The particles moved to the bottom of the bubble surfaces due to the flow around the bubble in the column. Figure 8b shows a pair of small bubbles attached to a single large ink particle.



9. Images of toner ink adsorption to a single suspended bubble in a sodium oleate solution at a pH of 9.5 (a) immediately after ink injection, (b) 5 min after injection, and (c) 25 min after injection.



10. Parameters used to calculate bubble surface coverage.

Figure 9 shows the accumulation of ink on a bubble surface with bubble residence time. Figure 9a shows a single suspended bubble (1.1 mm diameter) during a toner ink injection. Several ink particles are attached and have moved to the bottom of the bubble surface. Figure 9b shows a similar bubble, 5 minutes after an injection. Most of the surface area of the bubble is covered by ink. Figure 9c shows the same bubble from Fig. 9a, 25 min later. The bubble was completely covered by ink and toner networks (tails) have begun to accumulate on the bottom of the bubble.

#### Calculation of percentage of bubble coverage

We used image processing to estimate the percentage of bubble surface covered by toner ink. Figure 10 shows a sample image of a bubble partially covered with toner ink and a representation of the approximation used to calculate the area of bubble coverage. Values for the bubble radius,  $R$ , and for the distance,  $h$ , were measured on the image stills using

image processing software. The angle  $\alpha$  is determined from Eq. 3:

$$\alpha = \text{Arccos}\left(1 - \frac{h}{R}\right) \quad (3)$$

The area of bubble coverage  $A_c$  is equal to the sum of areas labeled A and B:

$$A_c = \text{area A} + \text{area B} = (\pi + \alpha)R^2 + R(R - h)\sin\alpha \quad (4)$$

The bubble coverage is the ratio (expressed as a percentage) of the area of adsorbed ink to the plane projected area of the bubble. This value is identical to the percent of bubble surface covered with ink. Figure 11 shows plots of the bubble coverage percentage with respect to residence time for similar sized bubbles in system solutions with fatty acid chemistry and a pH of 9.5. Each data point is the average percent coverage determined from three to four bubbles (with each bubble measurement consisting of several frames from a video sequence) and each point is accompanied by a representative image of those

used to calculate the percentage value. In Fig. 11a, bubbles quickly (within 15 s) reached a coverage of 30%. Bubble coverage then steadily increased until 100% coverage was achieved after approximately 4 min. Figure 11b shows a similar study for an oil-based offset ink; bubbles quickly became 15% covered. The bubble coverage then rose steadily and maximum bubble surface coverage occurred at 6.5 min of residence time.

#### Estimation of mass of attached ink

The mass of attached ink was estimated by approximating the volume of the ink shell (or ink layer) that wrapped a bubble. This ink shell volume  $V_{ink}$  was converted to a mass of ink  $m_{ink}$  by assuming a density of the ink in the shell layer.

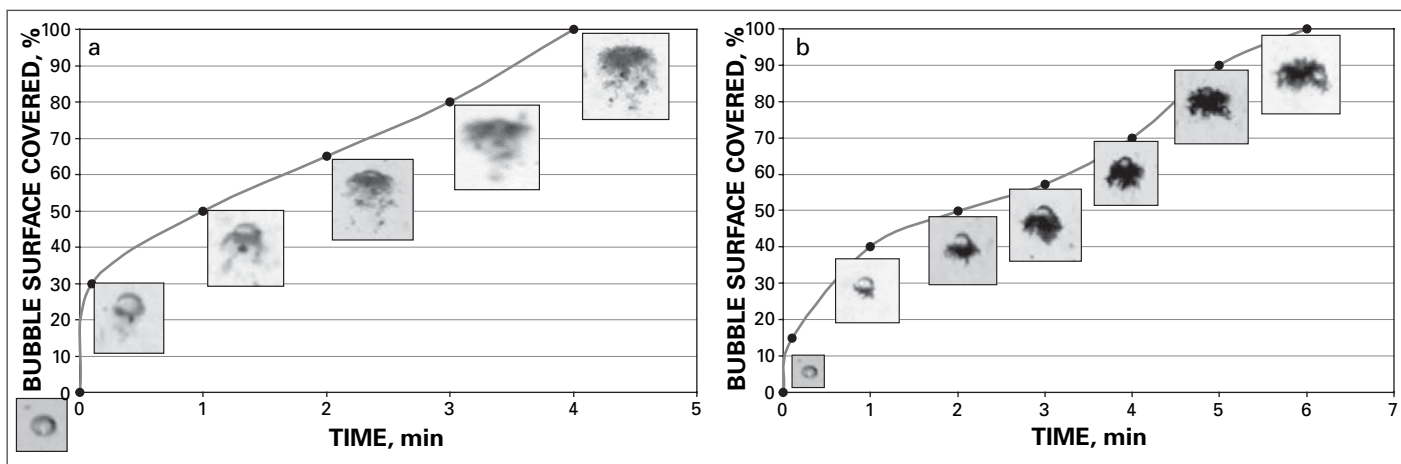
Image processing tools for “blob analysis” were used to find the area of the amorphous ink shell  $A_{blob}$  attached to a bubble. We calculated an effective radius that would yield a circle equal in area to the blob. Figure 12 and Eq. 5 illustrate this process:

$$R_{eff} = \sqrt{\frac{A_{blob}}{\pi}} \quad (5)$$

The spheroid shell volume of ink was determined by subtracting the bubble volume calculated from the bubble radius from the volume of ink and bubble calculated from the effective radius:

$$V_{ink} = \frac{4}{3} \pi (R_{eff}^3 - R_{bubble}^3) \quad (6)$$

For these measurements, the area of adsorbed ink was always larger than the plane projected area of the bubble. A similar procedure exists for quantification of ink adsorption when the amount of attached ink is small. The mass of ink was



11. a.) Percentage of bubble surface covered by toner ink in the suspending facility. b.) Percentage of bubble surface covered by offset ink in the suspending facility.

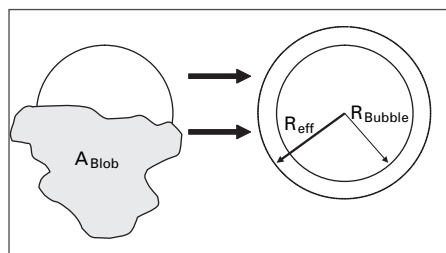
calculated by assuming the density of ink to be equal to that of water. Note that the volume of adsorbed ink is composed of some amount of ink and some amount of water. The fractional concentration of ink in the adsorbed ink,  $F_{Ink}$ , is unknown. We used Eq. 7 to determine the mass of ink adsorbed:

$$m_{Ink} = \tilde{n}_w \cdot F_{Ink} \cdot V_{Ink} \quad (7)$$

Figure 13 shows the attached toner ink mass with respect to time for three different assumed ink concentrations (50%, 75%, and 100%). The data points correspond to the bubble coverage and representative images shown in Fig. 11a. The mass of toner collected by 1 mm bubbles in calcium-soap chemistry increased with bubble residence time to 1.3 mg at 4 min, assuming a 50% adsorbed ink mixture. The mass of adsorbed ink did not reach a maximum value for the observed times, indicating that toner ink particles continued to attach to the ink shell network even after the bubble surface was fully covered. The growth and development of these networks appears to be a governing factor in the efficacy of the flotation process for toner inks.

## CONCLUSIONS

High magnification and high speed visualizations consistently showed that toner ink readily adsorbed to bubble surfaces in clear deionized water and in fatty-acid chemistries at pH of 9.5. Large planar toner particles adsorbed by small contact points. Stable networks of toner ink were observed for the calcium soap chemistry at a pH of 9.5. Adsorbed toner particles and toner networks were stable; desorption was not observed even for vigorous flows. We used image analysis to estimate percentage of bubble coverage and the mass of ink attached to a bubble. Bubbles



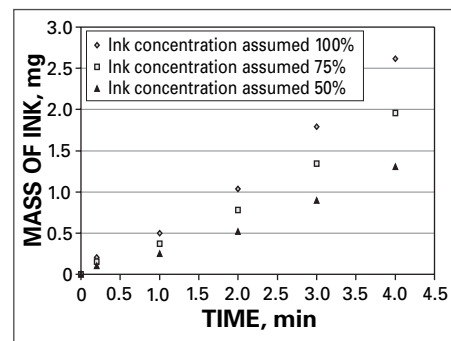
12. Calculation of effective radius from area of adsorbed ink.

with diameters of 1 mm were fully covered with ink after 4 min residence time. Initial estimates indicate that each bubble can carry more than 1 mg of toner ink.

A practical application of this work is that the stationary bubble facility and imaging system is fairly inexpensive and easy to operate, providing a replicable apparatus that can serve as a means of screening chemicals and ink types to determine the probability of ink attachment and extent of ink adsorption. The suspending bubble flow facility is more difficult to operate, but more closely simulates the operation of a flotation unit. Visualizations allow qualitative observations and quantitative estimates for ink and bubble interactions and flotation effectiveness. Studies are underway to determine the effect of bubble and ink particle size on flotation, the effect of enzymes on ink and bubble interactions [18], and further understanding of the toner network phenomena. **TJ**

## ACKNOWLEDGEMENTS

This work was supported by the Auburn Pulp and Paper Research and Education Center and the TAPPI Foundation. Thomas Bonometti is a doctoral student at L'Institut de Mécanique des Fluides de Toulouse (IMFT), France.



13. Mass of adsorbed toner for varying assumed ink concentrations.

## LITERATURE CITED

1. Davies, A.P.H., Rossi, L., and Duke, S.R., "A method for visualization and measurement of ink adsorption rates at bubble surfaces." *Fundamentals and Numerical Modeling of Unit Operations in the Forest Products Industry: AIChE Symposium Series*, Brogdon, B. (ed.). 324(96): 28(2000).
2. Davies, A.P.H. and Duke, S.R., *TAPPI J.* 1(3): 41(2002).
3. Emerson, Z.I., "Visualization of contaminants at bubble surfaces." Masters thesis: Auburn University, Auburn, Alabama, USA, 2003.
4. Ferguson, L.D., "Introduction to printing technology and ink chemistry." TAPPI Deinking Short-course, 1997.
5. Theander, K., and Pugh, R.J., *Colloids and Surfaces A: Physicochemical Engineering Aspects.* 240(1): 111(2004).
6. Azevedo, M.A.D., Drelich, J., Miller, J.D., *J. Pulp Paper Sci.* 25(9): 317(1999).
7. Dorris, G.M. and Page, M., *J. Pulp Paper Sci.* 23(5): 206(1997).
8. Doshi, M.R. and Dyer, J.M., *Paper Recycling Challenge Volume II: Deinking and Bleaching.* Doshi & Associates, Appleton, Wisconsin, 1997.

9. Doshi, M.R. and Dyer, J.M. Paper *Recycling Challenge Volume III: Process Technology*. Doshi & Associates, Appleton, Wisconsin, 1998.
10. Heindel, T., *TAPPI J.* 82(3): 115(1999).
11. Bloom, F., and Heindel, T.J., *Mathematical Computer Modeling*. 25(5): 15(1997).
12. Paulson, F.G., Berg, S.R., Vidotti, R.M., et al., *1997 Proceedings of the TAPPI Recycling Symposium*, TAPPI PRESS, Atlanta, Georgia, USA, p. 41.
13. Seifert, P., Gilkey, M., Scott, D., and McIntosh, R., *PaperAge*, 114(7): 11(1998).
14. Roizard, C., Poncin, S., Lapicque, F., et al., *Chem. Eng. Sci.* 54(13): 2317(1999).
15. Lee, H.L., Youn, H.J., Kim, J.M., Kim, J.W., "Evaluation of dynamic attachment phenomena of microstickies to air bubbles." *58<sup>th</sup> Appita Annual Conference and Exposition*. Proceedings. 21(2004).
16. Dorris, G.M., and Nguyen, N. "Flotation of model inks. Part II: Flexo ink dispersions without fibers." *J. Pulp Paper Sci.* 21(2): 55(1995).
17. Luttrell, G.H. and Yoon, R.H., "The effect of bubble size on fine particle flotation." *Mineral Processing and Extractive Metallurgy Review*. 5(2): 101(1989).
18. Ham, J.A., "Enzyme enhanced deinking of toner inks," Masters thesis: Auburn University, Auburn, AL, 2004.

Received: June 23, 2005  
 February 24, 2006  
 Accepted: February 27, 2006

This paper is also published on TAPPI's web site <[www.tappi.org](http://www.tappi.org)> and summarized in the April *Solutions! for People, Processes and Paper* magazine (Vol. 89 No. 4).

### INSIGHTS FROM THE AUTHORS

The Alabama Center for Paper and Bioresource Engineering (formerly the Auburn Pulp and Paper Research and Education Center) has a longstanding research program in paper recycling, particular in the areas of deinking, flotation, and membrane separations. The chemical engineering department here at Auburn has expertise and facilities for the optical studies of mass transfer, fluid dynamics, and separations. Thus, this research topic grew from our ongoing efforts to improve flotation processes and our interest in developing visualization methods that could be applied effectively for fundamental understanding of contaminant particle and bubble interactions.

We reported previously in *TAPPI J* on the development of the flow facilities and optical techniques for our flotation research, and their use for qualitative studies of flexographic and offset inks. The present research complements the previous work by expanding to studies of toner ink but also to furthering the visualization technique with higher speed visualizations and with ink adsorption quantification, such as the mass of adsorbed ink per bubble. These measurements allow results from our visualization to be compared with bench-top and mill scale flotation studies.

Determining how to quantify and measure features and observations revealed in the events and phenomena captured on video was the most difficult aspect of this research. We are addressing this by developing or applying effective image processing and image analysis methods.

Of all of the findings in this work, the most surprising were the observations of the development and stability of the toner (and offset) ink networks and complexes at bubble surfaces. The layer upon layer of ink at the bubble

surface resulted in much larger than anticipated amounts of ink particles, in terms of both number and mass, that adsorbed to individual bubbles. The highly stable attachment of particles to the bubble surface and to the networks was extremely interesting; no particles were ever seen to detach from the bubble surface or from each other once adsorbed.

Mills and chemical and equipment suppliers can use this information to revisit design and process practices with regard to bubble residence time because bubbles continue to collect toner and offset ink, even after the bubble surfaces are completely covered. More generally, mills and suppliers can use the optical techniques and bubble observation facilities to directly measure effects of process and chemistry variables on flotation effectiveness.

As we move forward with our work, we are continuing to apply these and other optical techniques to measure the effects of particle size and system chemistry on contaminant and bubble interactions in flotation systems. In particular, we are studying the role of calcium in the formation of the toner ink networks observed at bubble surfaces in this work.

---

Emerson, Bonometti, Krishnagopalan, and Duke are with the Department of Chemical Engineering Auburn University, Alabama 36849-5127 USA. Email Duke at [srduke@eng.auburn.edu](mailto:srduke@eng.auburn.edu).



Emerson



Bonometti



Krishnagopalan



Duke